Chapter

Characterization and Testing of High-Entropy Alloys from AlCrFeCoNi System for Military Applications

Victor Geanta and Ionelia Voiculescu

Abstract

High-entropy alloys (HEAs) can be obtained using various metallurgical processes such as vacuum arc remelting (VAR), induction melting, powder metallurgy, additive manufacturing, plasma sintering of powders, etc. Among these methods, the obtaining process in the VAR plant provides superior homogeneity characteristics for metal matrices, simultaneously with advanced purity, due to the high level of protection of the melts. The chapter presents a series of results on alloys with high entropy from the AlCrFeCoNi system, which can be used for various applications, including in the military field, for the realization of high-speed penetration protection panels. Experimental alloys were obtained by melting in electric arc under an argon atmosphere, using high-purity raw materials (greater than 99.5 wt%), and homogenization is ensured by successive five-times remelting of mini-ingots. The obtained alloys were subjected to microstructural analyses, mechanical tests, and also dynamic impact tests using incendiary perforation projectiles. At the same time, some tests were carried out on ballistic packages made of different materials, including high-entropy alloys. The results obtained in mechanical tests revealed high values of microhardness (over 600 $HV_{0.1}$) as well as compressive strengths above 2000 MPa. The mechanical characteristics of these alloys can undergo substantial changes by applying several heat treatments.

Keywords: high-entropy alloys, obtaining, characterization, dynamic testing

1. Introduction

High-entropy alloys (HEAs) are known for their special mechanical properties: high tensile strength resistance even at high temperature, high hardness, toughness exceeding that of most pure metals and alloys, comparable strength to that of structural ceramics and some metallic glasses, exceptional ductility and fracture toughness at cryogenic temperatures, and corrosion resistance. These specific properties were mainly attributed to complex concentrated solid solutions formed by the suppression of fragile intermetallic compounds as a result of high mixing entropy and enthalpy values [1]. HEAs generally tend to form single-phase solid solutions in the case of low mixing enthalpy and atomic size difference. Generally speaking, the formation of a single-phase solid solution corresponds to the mixing enthalpy values (DHmix) situated in domain of -15 kJ/mol < DHmix <5 kJ/ml and $0 < \delta < 5$ [2].

As a result of these special features, HEA is currently an alternative to use as material for a number of special areas, such as structural applications; aerospace engineering and civil transportations; superconducting electromagnets such as magnetic resonance imaging, scanners, nuclear magnetic resonance machines, and particle accelerators; high-temperature applications such as gas turbines, rocket nozzles, and nuclear construction; cryogenic applications such as rocket casings, pipework, and liquid O_2 or N_2 equipment; refractory elements such as Nb, Mo, and Ta that can maintain their high strength even above 1200°C, superior to traditional super alloys such as Inconel 718 and Haynes 230; hardfacing applications; and military applications.

The specifications on the security of collective protection equipment and structures in the military field set forth enhanced requirements for the resistance of the protection panels/floors/elements against the penetration by various types of projectiles, due to the diversification of the types of interventions in the military activities.

The main characteristics of the materials intended for the manufacture of protection components are as follows: the highest possible breaking and yield strength values, the highest possible hardness and impact resistance, and the highest possible elongation at break and energy absorbed by a notched specimen while breaking under an impact load (the Charpy test) at temperatures down to minus 40°C. The current military specifications recommend hardness values of at least 540–600 BHN (Brinell hardness) or 55–60 HRC (Rockwell hardness) and, for strength characteristics, such as the yield strength, values above 1500 and 1700 MPa for the breaking strength. In the case of the impact fracture energy using the Charpy test, the values must be of approximately 13 J at −40°C, with elongations of at least 6% [3].

Such requirements have been met by designing metallic alloys of various compositions; the most widely used is the high-strength microalloyed steels, used to produce reinforcement elements of thicknesses between 8.5 and 30 mm. Some research papers in the military field [4] have shown that the hardness of the plating material is not a sufficient factor to provide maximum resistance against penetration by projectiles, considering that the values of the mechanical strengths (yield and breaking) are much more important in the behavior process under dynamic stress.

Accurate measurements of dynamic stresses during impact stress have detected mechanical stress values of 28 GPa in the case of bainitic microstructure steels, while in the case of static stress, the measured stresses were of no more than 2 GPa [5].

A ballistic performance index (BPI) [6, 7] was also proposed to estimate the ballistic strength of armored plates, containing data on steel density, the elastic modulus, yield and tensile strength, Poisson's coefficient, and the constriction or elongation during impact tests. There are terms that contain elastic and plastic deformation components, as well as terms that take into account the kinetic energy of the target-projectile system after impact. Therefore, the main characteristics that

Alloy	Yield strength, MPa	Compressive strength, MPa	Plastic deformation, %
AlCrFeCoNi	1250.96	2004.23	32.7
CrFeCoNiCuTi	1272	1272	1.6
AlCrMnFeCoNiCuTiV	1862	2431	0.95
$CrFeCoNiCuTi_{0.5}$	700	1650	21.26

Table 1.
Mechanical properties of some high-entropy alloys [8].

metallic materials used in special military applications need to feature for the best impact behavior are as follows:

- The highest possible hardness, as a measurement of the solid material's resistance against the penetration of its surface by various types of penetrators, with permanent shape changes, when a static or dynamic force is applied to them; the macroscopic hardness is generally characterized by the nature and strength of the intermolecular bonds, and the behavior of the solid material under the action of force is complex.

- Toughness, which describes the capacity of a metallic material to absorb the breaking energy, the strength of its metallic matrix when various cracks occur and propagate, and the energy of forming the breaking surfaces, considering that the breaking occurs by consuming the impact stress energy, with local plastic deformation.

- Impact strength, which is the relative susceptibility to breaking by the action of forces applied at high velocity.

High-entropy alloys from the AlCrFeCoNi system feature very good mechanical properties for military applications, as shown in **Table 1**. Thus, the yield stress, the compressive strength, and the plastic deformation of these alloys reach unexpected values [8–20], making them usable as composite structures, resistant to dynamic stresses with high deformation velocity, applicable in the field of collective protection [9–20].

2. Obtaining of $Al_xCr_yFe_zCo_vNi_w$ class of high-entropy alloys

The most commonly used method for successfully producing high-entropy alloys is the electric arc melting of the load materials in a vacuum arc remelting equipment (with current values of up to 500 A) in controlled atmosphere. The main technological operations pursued in this case are presented below.

2.1 Obtaining AlCrFeCoNi alloys in vacuum arc remelting furnace

Special type of materials chosen for making the ballistic target is experimental alloys AlCrFeCoNi, obtained in vacuum arc remelting equipment (MRF ABJ 900, in ERAMET Laboratory, University Politehnica of Bucharest, Romania). For calculating the metallic load, the theoretical degrees of assimilation of the elements in the melt and of the possible vaporization losses during the metallurgical process in vacuum or in argon-controlled atmosphere must be taken into account (**Figure 1**).

Mass losses are estimated on the basis of the literature data thereon, the degree of oxidation of the metallic load materials, the characteristics of the elements in the load, their positioning in the series of electrochemical potentials, the characteristics of the preparation aggregate, and the experience in the preparation process. It should be noted that the metallic load used to obtain high-entropy alloys must be of high quality, low in phosphorus and sulfur, and degreased and properly machined (in terms of granulometry). The degree of purity of the elements the alloy is over 99%. The elements dosed in equimolecular or quasi-equimolecular proportions are introduced following an order determined according to the type of alloy to be prepared, into the crucibles in the copper plate, water-cooled throughout the metallurgical process.

In order to produce high-entropy alloys under high-purity conditions, the working chamber must be suitably prepared by successive vacuuming and argon purging

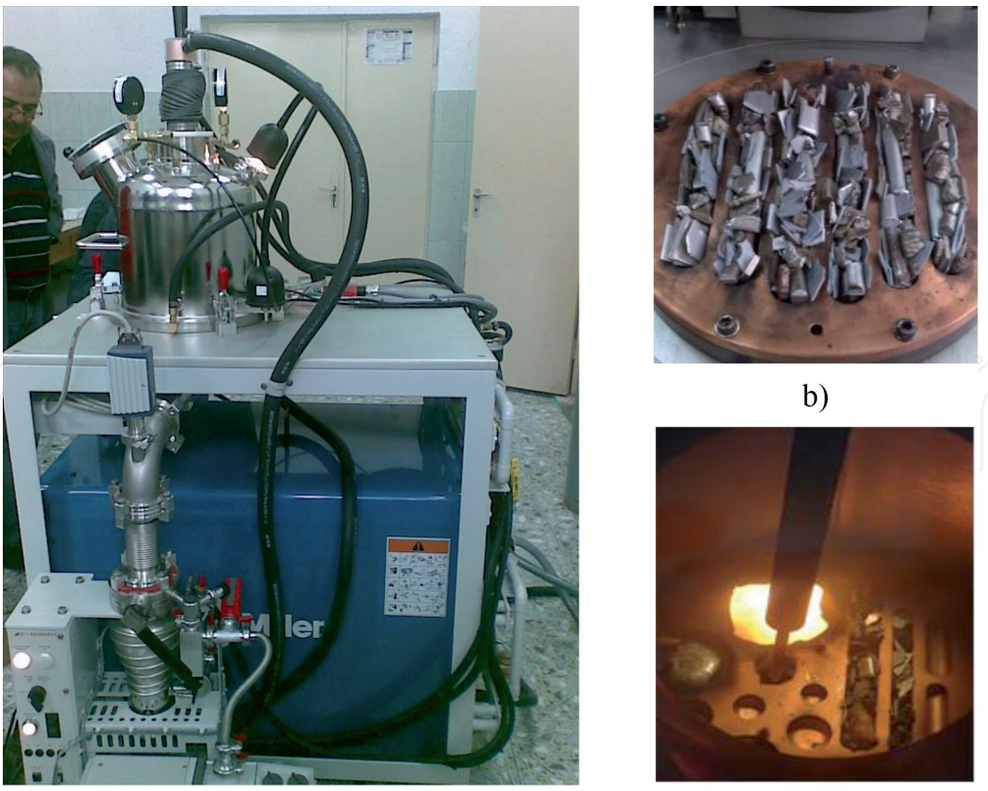

a) b) c)

Figure 1.
Vacuum arc remelting equipment MRF ABJ 900 and working chamber, in ERAMET Laboratory, University Politehnica of Bucharest, Romania.

operations performed at least three times. The vacuuming is performed using preliminary vacuum systems and diffusion pumps, which can provide pressure levels of about 3.5–4 × 10^{-4} mbar. Pure argon (Ar 5.3, 99.99%) is used for purging and melting. These operations provide a maximum oxygen content of 40–60 ppm in the working chamber. The final stage of the process is the argon purging of the working chamber and the setting of a working pressure level slightly above the atmospheric pressure.

The process of producing high-entropy alloys consists in melting the load materials, followed by the remelting of the samples for five to seven times, turning them on opposite sides to ensure a fully alloyed state and to improve the chemical homogenization of the mini-ingots. The entire preparation process is carried out by electric arc remelting in argon-controlled atmosphere.

The melting mode of the vacuum arc remelting furnace must be adapted to the type of alloy being prepared. These parameters vary during the preparation process, depending on the stages and the activities being carried out. The thorium tungsten electrode must be shifted during melting so that it is approximately 1/4" away from the copper plate electrode, and the electric arc formed sweeps the entire surface of the load for complete homogenization. Following melting and solidification, mini-ingots of weights almost constant compared to that of the load introduced into the VAR are produced.

Using this method, experimental high-entropy alloys have been instantaneously cooled by forced cooling of the water pumped at the base of the copper plate (the crystallizer of the furnace).

The melted material solidifies ultrafast in the water-cooled copper shell. The mini-ingots produced can have different shapes, depending on the shape of the cavity in the copper plate of the furnace. The samples were analyzed, according to the chemical composition, in order to define their physical, chemical, mechanical, etc. properties.

Figure2.
Metallic molds for casting $Al_{0.8}CrFeCoNi$ alloy.

The chemical compositions of the metallic materials used are as follows:

- Extra soft steel, MK3 grade: C = 0.02 wt%; Si = 0.04 wt%; Mn = 0.21 wt%; S = 0.02 wt%; P = 0.015 wt%; Ni = 0.2 wt%; Cr = 0.15 wt%; Mo = 0.07 wt%; Cu = 0.14 wt%; Al = 0.12 wt%; Fe = ballance wt%
- Metallic chromium with 99 wt% Cr
- Electrolytic aluminum with 98.5 wt% Al
- Metallic cobalt with 99.5 wt% Co
- Electrolytic nickel with 99.5 wt% Ni

2.2 Obtaining of AlCrFeCoNi alloy in duplex system including induction and vacuum arc remelting furnace

A vacuum induction melting-vacuum arc remelting (VIM-VAR) duplex technology was selected to produce the high-entropy alloy AlCrFeCoNi in order to increase the purity of the alloy and to improve its mechanical properties. The experimental batches were prepared in the vacuum induction melting furnace Balzers, HU-40-25-40-04 type, with a capacity of 12 kg and in the MRF ABJ 900 vacuum arc remelting equipment, both from the ERAMET Laboratory, Bucharest.

The high-entropy alloy used to make the ballistic protection plates in the vacuum induction furnace was produced according to a classical preparation technology, using highly pure materials, and metallic molds made of iron Fc 250 (**Figure 2**) were used for casting to ensure the production of 150 × 100 × 10 mm rectangular plates.

The load calculation (based on the molar mass of the chemical elements, M_{mol}) for obtaining the $Al_{0.8}CrFeCoNi$ alloy, taking into account the estimated elemental losses, is as follows (Eq. (1)):

$$M_{mol} = 27x0.8 + 52 + 56 + 59 + 59 = 247.6 \text{ g} \quad (1)$$

The concentration (% weight) of the alloying elements in the alloy was Al = 8.72 wt%; Cr = 21 wt%; Fe = 22.62 wt%; Co = 23.83 wt%; and Ni = 23.83 wt%. The alloy mass calculated based on the volume and density of the alloy cast in a plate and

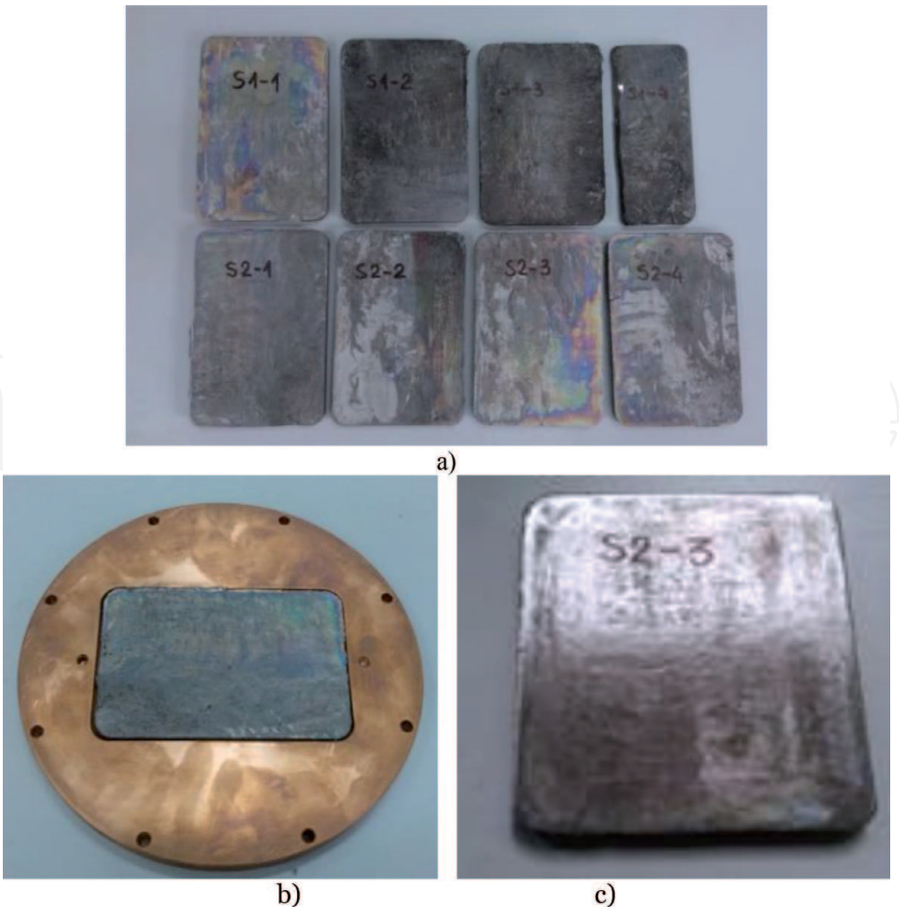

Figure 3.
HEA $Al_{0.8}CrFeCoNi$ alloy plates obtained by VIM-VAR technology. (a) As-cast HEA samples obtained by VIM technology; (b) HEA sample positioned in copper plate of VAR equipment to be remelted; (c) sample after remelting procedure in VAR equipment.

related network was 1.111 and 0.574 kg, respectively, resulting in an alloy quantity of approx. 1.6855 kg per ingot.

Since alloy losses occur due to oxidation, due to the interaction with the furnace walls and to the casting ladle, a quantity of 8 kg of prepared alloy is considered per batch.

The quantities of materials used for each batch, also taking into account the oxidation losses, are as follows: Al = 0.74 kg; Cr = 1.70 kg; Fe = 1.85 kg; Co = 1.95 kg; and Ni = 1.93 kg. The total weight of the batch was of 8.17 kg. The $Al_{0.8}CrFeCoNi$ alloy plates obtained by casting are shown in **Figure 3**.

The production of the HEA $Al_{0.8}CrFeCoNi$ plates was completed by refining in the vacuum arc remelting furnace, for which, based on the requirements of the military field, a special copper plate was made, according to **Figure 2b**.

The working procedure in the VAR furnace was classical, seeking the most efficient homogenization of the alloy to ensure the best possible mechanical properties, by remelting each sample three times on each side (**Figure 3c**).

3. Mechanical tests

3.1 Impact fracture tests

The impact fracture tests were performed using a Charpy pendulum, to measure the energy absorbed in the process of dynamic fracture of standardized (notched)

specimens. The values resulting from the impact fracture test for some AlCrFeCoNi alloys are shown in **Table 2**.

As can be seen from the values of the breaking energy shown in the table, the experimental materials have a tenacity corresponding to structural steels, while the hardness values are similar to those of tool steels.

3.2 Microhardness

The hardness of the experimental materials was determined using the Shimadzu HMV2T microhardness apparatus in Lamet Laboratories from *Politehnica* University of Bucharest. The measurements were made in line, with mark distances of about 500 μm, using the fingerprint force of 0.1 N and pressing time of 10 seconds [9–12]. For the $Al_xCr_yFe_zCo_vNi_w$ system, the entire spectrum of microhardness values in the x = y = z = v = w = 0.2 ... 2 at% range was analyzed, as shown in **Figure 4**.

The coding of the samples in **Figure 4** was based on the atomic proportions of the chemical elements; thus, HEA 1 = AlCrFeCoNi; HEA 2 = $Al_{1.5}$CrFeCoNi; HEA 3 = Al_2CrFeCoNi; HEA 5 = $Al_{0.8}$CrFeCoNi; HEA 6 = $Al_{0.6}$CrFeCoNi; HEA 7 = $Al_{0.4}$CrFeCoNi; HEA 8 = $Al_{0.2}$CrFeCoNi; HEA 9 = $Al_{1.2}$CrFeCoNi; and HEA 10 = $Al_{1.4}$CrFeCoNi. The maximum hardness value was obtained for the sample HEA 3, with maximum concentration of aluminum.

The coding of the samples in **Figure 5** was based on the atomic proportions of the chemical elements; thus, HEA 11 = AlCrFeCo$Ni_{1.2}$; HEA 12 = AlCrFeCo$Ni_{1.4}$; HEA 13 = AlCrFeCo$Ni_{1.6}$; HEA 14 = AlCrFeCo$Ni_{1.8}$; HEA 15 = AlCrFeCoNi_2; HEA 16 = AlCrFeCo$Ni_{0.8}$; HEA 17 = AlCrFeCo$Ni_{0.6}$; HEA 18 = AlCrFeCo$Ni_{0.4}$; and HEA 19 = AlCrFeCo$Ni_{0.2}$. The maximum hardness value was obtained for the sample HEA 11.

Test no.	Impact energy, J				
	HEA 1	HEA 5	HEA 6	HEA 12	HEA 14
1	62.1	67.1	67.0	66.0	62.4
2	62.7	67.2	66.9	65.8	62.3
3	62.1	67.0	67.1	65.9	62.1
4	62.2	67.3	68.9	66.1	62.1

Table 2.
Impact fracture energy values for some experimental HEAs.

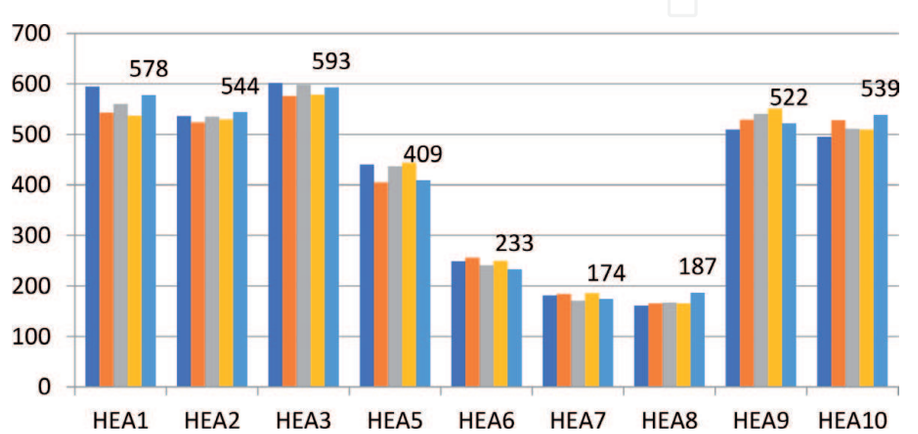

Figure 4.
Microhardness $HV_{0.1}$ values for experimental HEA 1 to HEA 10.

The coding of the samples in **Figure 6** was based on the atomic proportions of the chemical elements; thus, HEA 20 = $AlCrFeCo_{0.8}Ni$; HEA 21 = $AlCrFeCo_{0.6}Ni$; HEA 22 = $AlCrFeCo_{0.4}Ni$; HEA 23 = $AlCrFeCo_{0.2}Ni$; HEA 24 = $AlCrFeCo_{1.2}Ni$; HEA 25 = $AlCrFeCo_{1.4}Ni$; HEA 26 = $AlCrFeCo_{1.6}Ni$; HEA 27 = $AlCrFeCo_{1.8}Ni$; and HEA 28 = $AlCrFeCo_{2}Ni$. The maximum hardness value was obtained for the sample HEA 26.

The coding of the samples in **Figure 7** was based on the atomic proportions of the chemical elements; thus, HEA 29 = $AlCr_{0.2}FeCoNi$; HEA

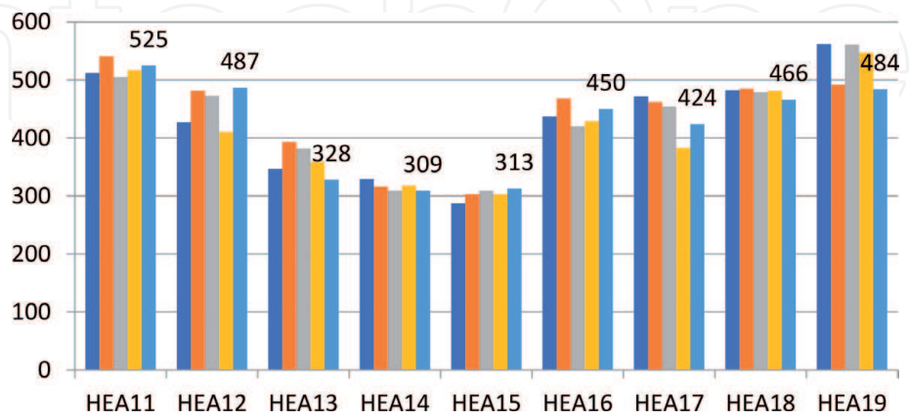

Figure 5.
Microhardness $HV_{0.1}$ values for experimental HEA 11 to HEA 19.

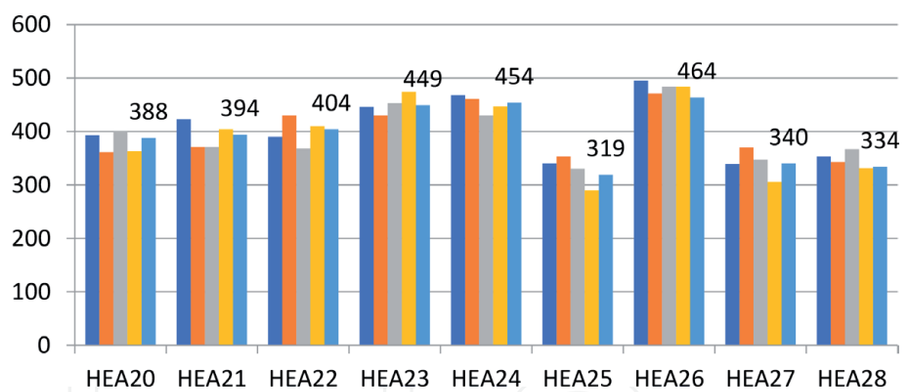

Figure 6.
Microhardness $HV_{0.1}$ values for experimental HEA 20 to HEA 28.

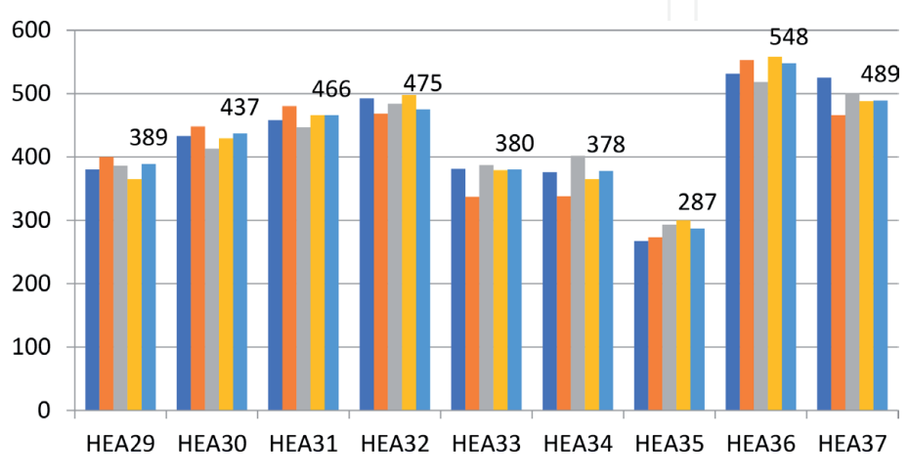

Figure 7.
Microhardness $HV_{0.1}$ values for experimental HEA 29 to HEA 37.

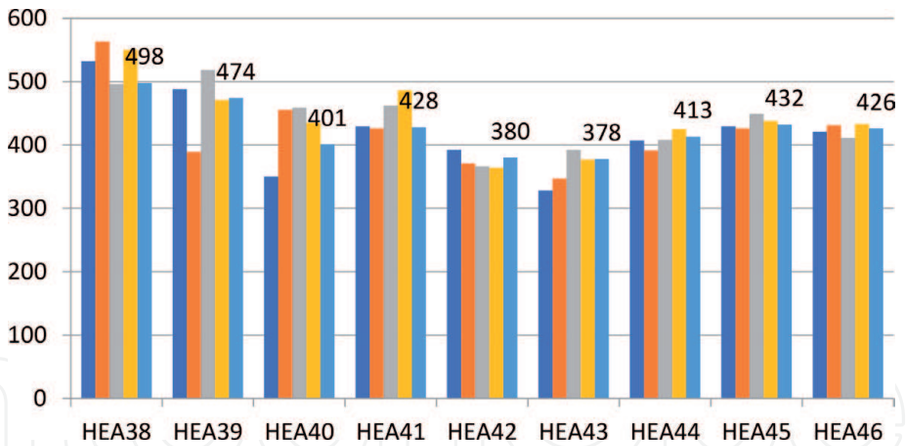

Figure 8.
Microhardness $HV_{0.1}$ values for experimental HEA 38 to HEA 46.

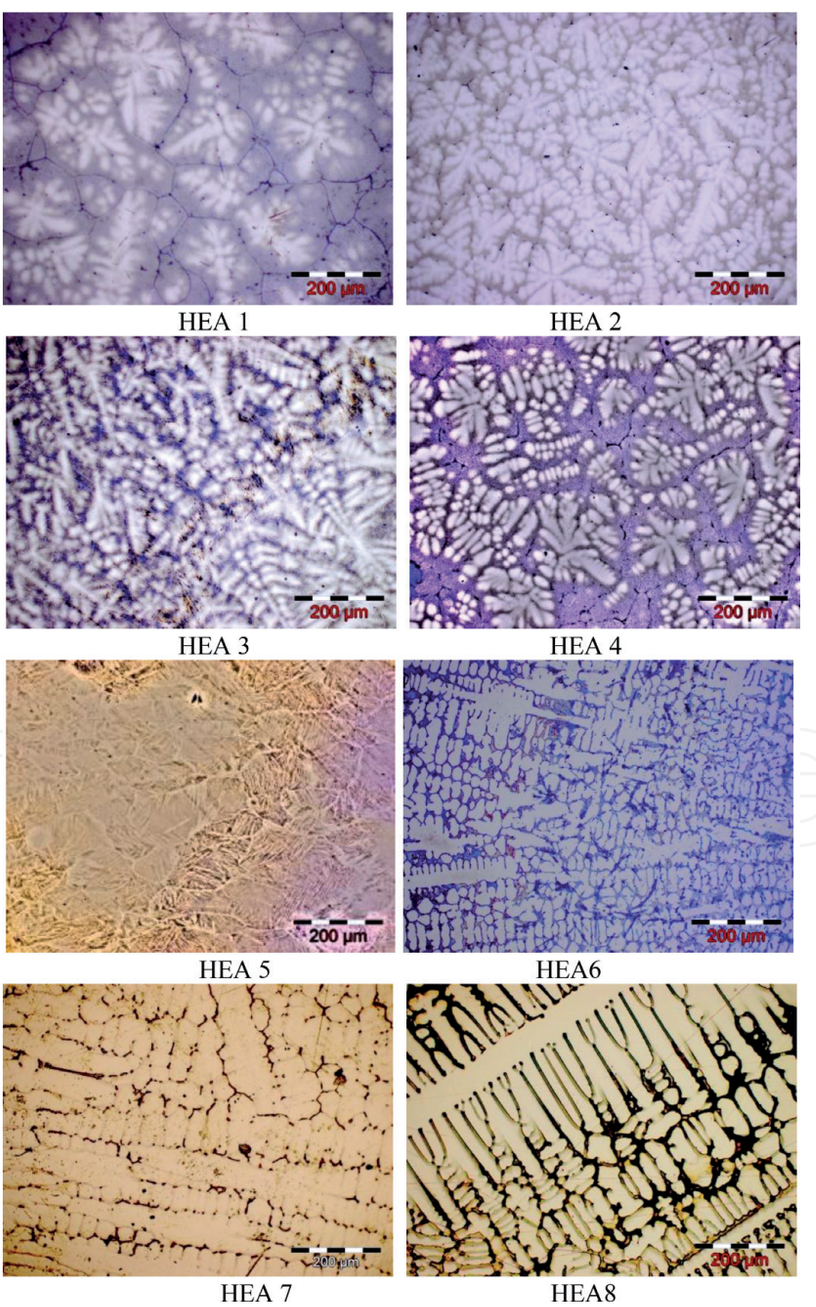

Figure 9.
Experimental as-cast $Al_xCrFeCoNi$ alloys.

30 = $AlCr_{0.4}FeCoNi$; HEA 31 = $AlCr_{0.6}FeCoNi$; HEA 32 = $AlCr_{0.8}FeCoNi$; HEA 33 = $AlCr_{1.2}FeCoNi$; HEA 34 = $AlCr_{1.4}FeCoNi$; HEA 35 = $AlCr_{1.6}FeCoNi$; HEA 36 = $AlCr_{1.8}FeCoNi$; and HEA 37 = $AlCr_2FeCoNi$. The maximum hardness value was obtained for the sample HEA 36.

The coding of the samples in **Figure 8** was based on the atomic proportions of the chemical elements; thus, HEA 38 = $AlCrFe_{0.2}CoNi$; HEA 39 = $AlCrFe_{0.4}CoNi$; HEA 40 = $AlCrFe_{0.6}CoNi$; HEA 41 = $AlCrFe_{0.8}CoNi$; HEA 42 = $AlCrFe_{1.2}CoNi$; HEA 43 = $AlCrFe_{1.4}CoNi$; HEA 44 = $AlCrFe_{1.6}CoNi$; HEA 45 = $AlCrFe_{1.8}CoNi$; and HEA 46 = $AlCrFe_2CoNi$. The maximum hardness value was obtained for the sample HEA 38, for minimum concentration of iron.

4. Microstructure

The microstructure of experimental high-entropy alloys was performed selectively by optical microscopy (Olympus GX51 reversed optical microscope) and scanning electron microscopy (Inspect SEM, FEI Company, scanning electron microscope equipped with EDAX Z2e detector) [9, 13–16]. The microstructural aspect of some experimental alloys is shown in **Figures 9–14**.

All materials show dendritic formations and interdendritic precipitations in experimental as-cast HEAs. Some of them (HEA 5) shows polyhedral grains and acicular phase growth from the grain boundary (**Figure 9**). The images have been performed for the same magnification (scale of 200 μm). The sample HEA 15 with the highest nickel concentration has the orientation and sequence of the alpha and gamma phases, in the form of parallel or perpendicular planes (**Figure 10**).

Changing the Co content does not make changes to the microstructure, which has a dendritic appearance (**Figure 11**). The increase in chromium content resulted

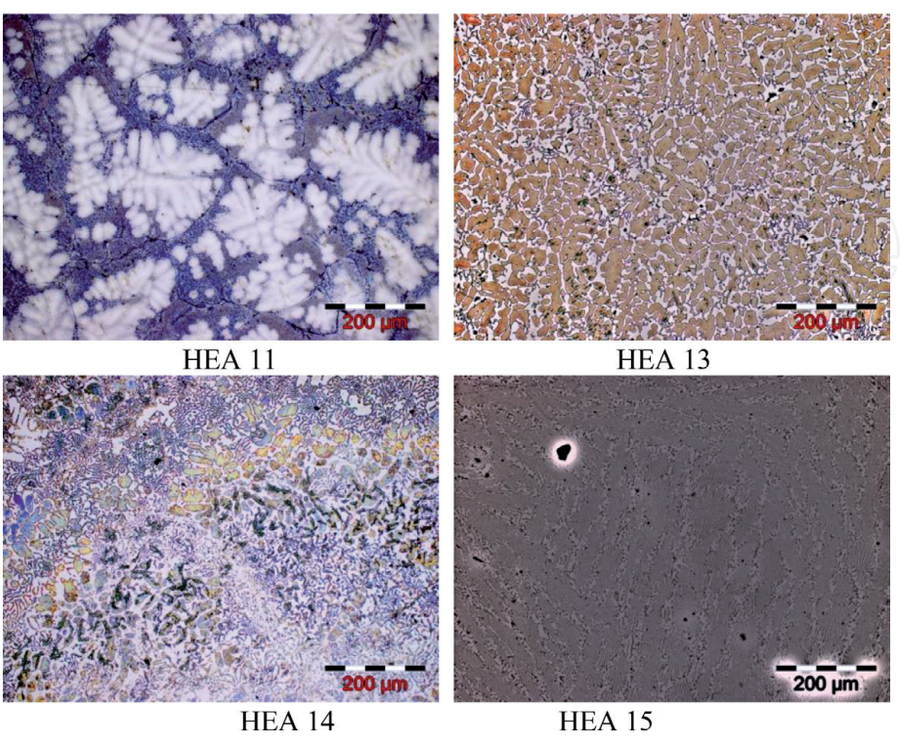

Figure 10.
Experimental as-cast AlCrFeCoNix alloys.

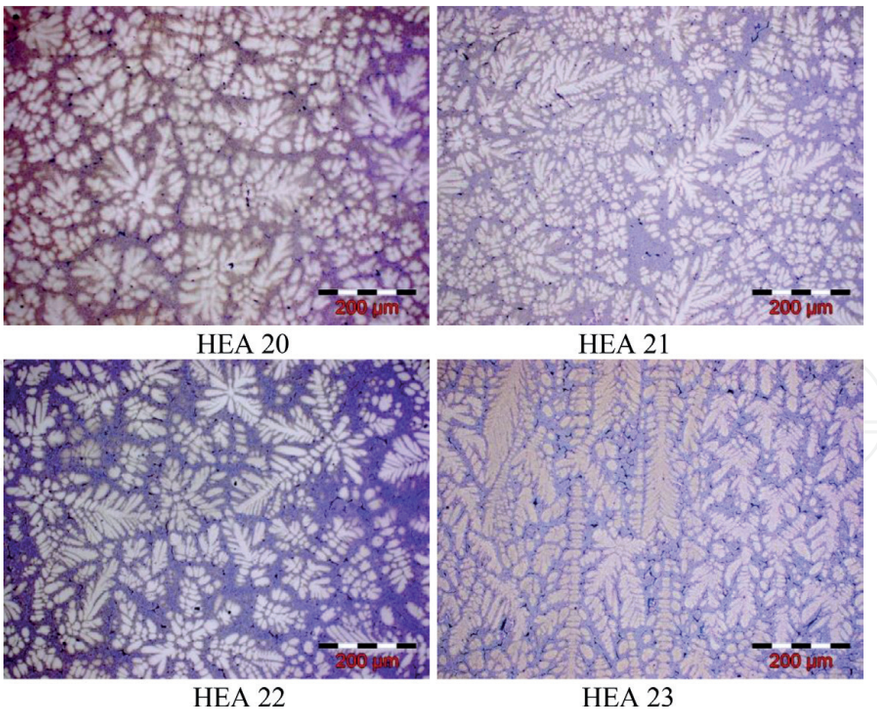

Figure 11.
Experimental as-cast AlCrFeCo$_x$Ni alloys.

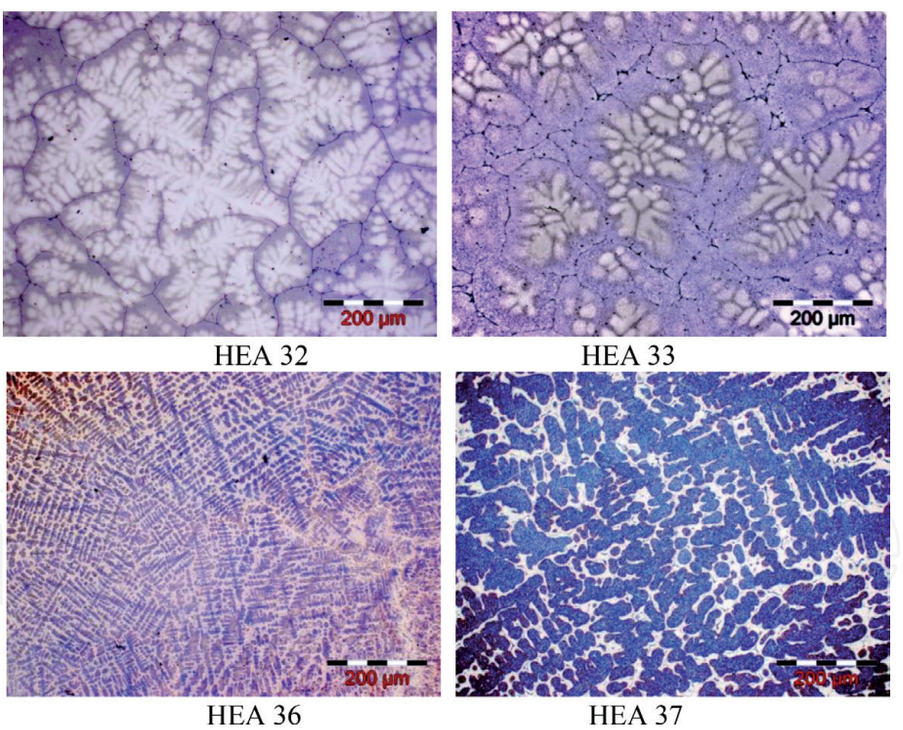

Figure 12.
Experimental as-cast AlCr$_x$FeCoNi alloys.

in an increased finishing of dendritic microstructure granulation for HEA 36 sample, which also led to an increase in hardness (**Figure 12**).

Scanning electron microscopy images revealed the fine and nanostructured microstructure with polyhedral grains and the layout of phases in quasi-parallel planes (**Figure 13**) [15].

In the case of high-Ni samples, higher magnification powers can be seen in phase configurations, in acicular or polymorphic form (**Figure 14**).

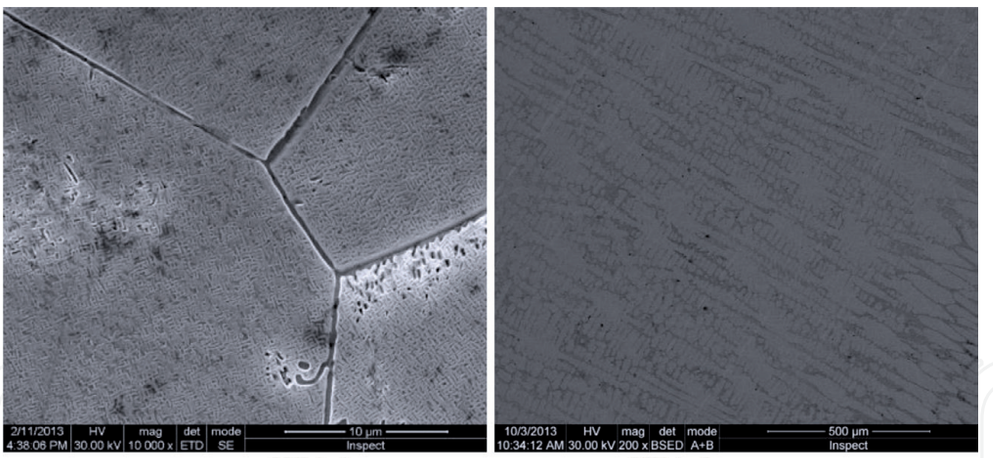

Figure 13.
SEM images of $Al_xCrFeCoNi$ alloys.

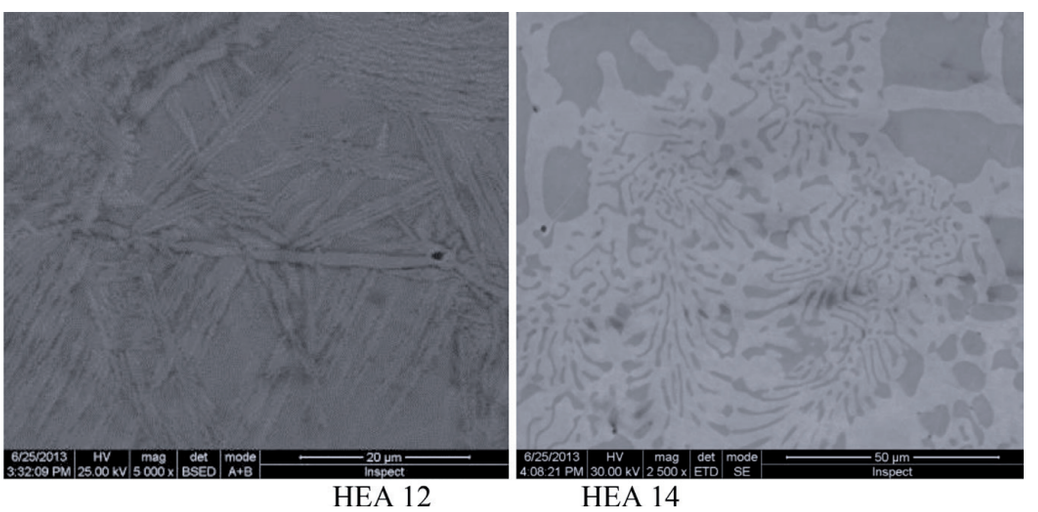

Figure 14.
SEM images of $AlCrFeCoNi_x$ alloys.

5. Dynamic testing

Several ballistic packages (**Figure 15**) were made for the testing of composite structures at high-velocity perforation, explosion, and high-velocity deformation. The packages have a sandwich structure, containing aluminum, steel, or ceramic plates or polymer HEA plate and, finally, aluminum plate again. The images from the firing room and the testing configuration are shown in **Figure 16**, and the experimental stand scheme for dynamic test is shown in **Figure 17**.

The ballistic packages undergoing tests for checking the bullet impact behavior were fastened to a wooden stand at a distance of 5 m from the machine-gun barrel's muzzle. The amount of powder in the cartridge shell was varied in order to obtain the desired initial velocity [15–19].

Two 7.62 × 39 mm incendiary armor-piercing bullets with initial velocities of 660 and 728 m/s, respectively, were fired at the targets. The ballistic package resisted punching for the first fire (**Figure 17a**) and then perforated at the second firing (**Figure 17b**).

The same procedure of dynamic testing, using 7.62 × 39 mm incendiary armor-piercing bullets at initial velocities of 723 and 728 m/s, respectively, was applied at

the HEA-ceramic ballistic package. This type of ballistic package was perforated both at the first and second cases (**Figure 18**).

The last procedure was applied using 7.62 × 39 mm incendiary armor-piercing bullets at initial velocities of 720 and 725 m/s, respectively, for dynamic testing of HEA-ceramic ballistic package. This type of ballistic package was entirely perforated, in both cases (**Figure 19**).

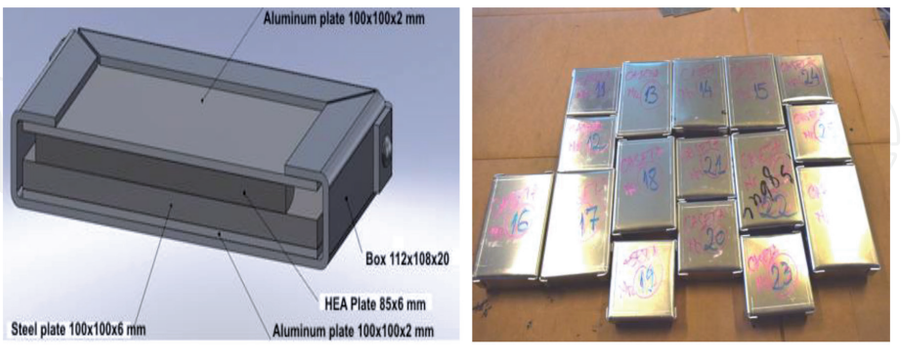

a) b)

Figure 15.
Ballistic packages prepared for dynamic tests.

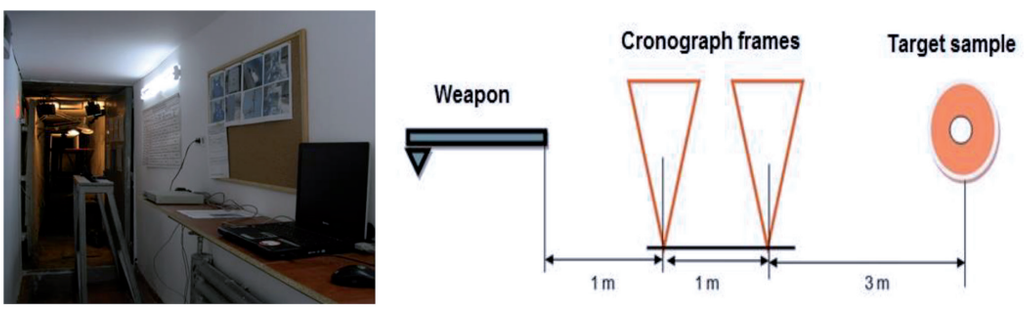

a) b)

Figure 16.
Firing room and experimental stand for dynamic test.

a) b)

Figure 17.
HEA-steel ballistic package during dynamic tests (a) after the first firing and (b) after the second firing.

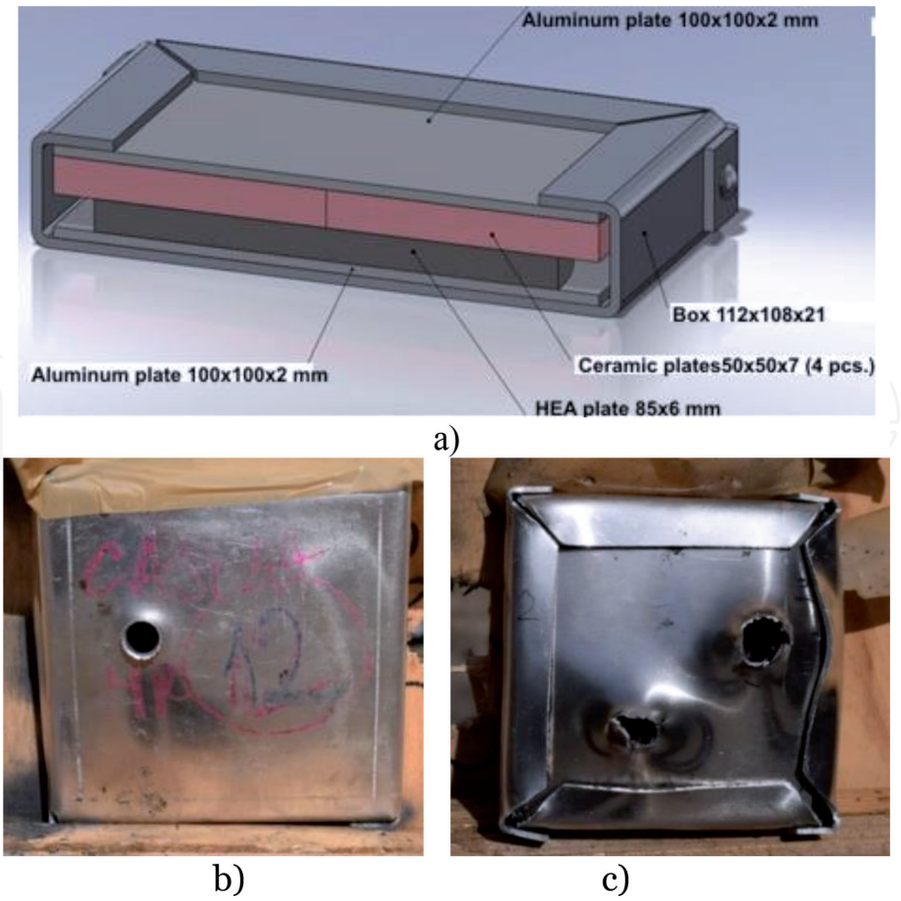

Figure 18.
HEA-ceramic ballistic package during dynamic tests (a) after the first firing (b) and after the second firing (c).

Figure 19.
HEA-polymer ballistic package during dynamic tests. (a) after the first firing and (b) after the second firing.

6. Conclusions

High-entropy alloys are well suited for production in vacuum arc remelting furnaces due to low material losses and to obtaining high purity by working in vacuum and argon. Moreover, they can also be produced in induction furnaces, for superior purity, using the VIM-VAR duplex process.

The hardness decrease of the AlCrFeCoNi class high-entropy alloys is proportional to the aluminum content decrease, from 500 HV_1 for HEA 1 (AlCrFeCoNi) at 400 HV_1 for HEA 5 ($Al_{0.8}$CrFeCoNi) and 224 HV_1 for HEA 6 ($Al_{0.6}$CrFeCoNi).

The hardness decrease can be explained by the reduction in the quantity and number of hard precipitates (Fe-Al compounds) in the metallic matrix.

The hardness further decreases by increasing the nickel content, which allows the formation of face-centered cubic (FCC) solid solutions of low hardness and high tenacity. In this type of solid solution the chemical elements have a good solubility, with a low tendency of separation of hard and brittle compounds.

The fracture energy values are in the range of 62–67 J for all five types of alloys, as the hardness oscillates in the range 200–500 $HV_{0.1}$. As a result, the hardening effect is not manifested by decreasing the metal matrix toughness in the case of high-entropy alloys in the analyzed alloy class.

The microstructure of high-entropy alloys is virtually "frozen" at the melt, with the solution retaining a conglomerate of chemical elements which are oftentimes very different (iron-related elements such as Cr, Ni, and Co, which together form solid solutions along with aluminum, a transition metal whose solubility greatly differs from that of Fe, Cr, Ni, and Co). The cooling condition creates entropy with very high values and explains the obtaining of completely different characteristics compared to the alloy cooled at usual rates.

Depending on the share of the alloying elements, one or two types of solid solutions are formed, partially embedding the other alloying elements. The dendritic microstructure predominates, separating into acicular compounds or globular precipitates, depending on the chemical composition and the cooling rate.

The tests on the behavior of high-entropy alloys at strong impacts were conducted under identical conditions. In the case of ballistic packages resistant at high-velocity penetration impacts, the best option is the HEA-steel system. High-entropy alloys, according to their composition, can be used in various sectors: medical engineering, earthwork equipment, and ballistic packages for individual and collective protection.

Acknowledgements

This paper was supported by the Romanian National Authority for Scientific Research CNDI-UEFISCDI, project number PN-III-P1-1.2-PCCDI-2017-0875 – PCCDI 20-2018 (HEAPROTECT).

Thanks

The authors want to thank the team of researchers coordinated by Professor PhD Tudor Cherecheş for collaborating in the dynamic tests and the processing of experimental data.

Author details

Victor Geanta and Ionelia Voiculescu*
Ionelia Voiculescu, University Politehnica of Bucharest, Bucharest, Romania

*Address all correspondence to: ioneliav@yahoo.co.uk

References

[1] Yeh J, Chen SK, Lin S, Gan JY, Chin TS, Shun TT, et al. Nanostructured high entropy alloys with multiple component elements: Novel alloy design concepts and outcomes. Advanced Engineering Materials. 2004;**6**:299-303

[2] Zhang Y et al. Microstructure and properties of high entropy alloys. Progress in Materials Science. 2014;**61**:1-93

[3] Maweja K, Strumpf W. The design of advanced performance high strength low-carbon martensitic armor steels microstructural considerations. Materials Science and Engineering A. 2008;**480**:160-166

[4] Maweja K, Strumpf W. Fracture and ballistic-induced phase transformation in tempered martensitic low-carbon armour steels. Materials Science and Engineering A. 2006;**432**:158-169

[5] R.I. Hammond, W.G. Proud. Does the pressure-induced α–ε phase transition occur for all low-alloy steels? Proceedings of the Royal Society of London A. 2004;**460**:2959-2974

[6] Srivathsan B, Ramakrishnan N. Ballistic performance maps for thick metallic armour. Journal of Materials Processing Technology. 1999;**96**:81-91

[7] Srivathsan B, Ramakrishnan N. A ballistic performance index for thick metallic armour. International Journal of Modeling, Simulation, and Scientific Computing. 1998;**3**:33-40

[8] Wang YP, Li BS, Ren MX, Yang C, Fu HZ. Microstructure and compresive properties of AlCrFeCoNi high entropy alloy. Materials Science and Engineering A. 2008;**491**:154-158

[9] Voiculescu I, Geanta V, Vasile IM, Ştefănoiu R, Tonoiu M. Characterisation of weld deposits using as filler metal a high entropy alloy. Journal of Optoelectronics and Advanced Materials. 2013;**15**(7-8):650-654

[10] Geantă V, Voiculescu I, Miloșan I, Istrate B, Mateș IM. Chemical composition influence on microhardness, microstructure and phase morphology of AlxCrFeCoNi high entropy alloys. Revista de Chimie (Bucharest). 2018;**69**(4):798-801

[11] Geantă V, Voiculescu I, Stefănoiu R, Chereches T, Zecheru T, Matache L, et al. Dynamic impact behaviour of high entropy alloys used in the military domain. Euroinvent ICIR 2018 IOP Publishing IOP Conference Series: Materials Science and Engineering 2018;**374**:012041. DOI: 10.1088/1757-899X/374/1/012041

[12] Geantă V, Voiculescu I, Istrate B, Vrânceanu D, Ciocoiu R, Cotruț C. The influence of chromium content on the structural and mechanical properties of AlCrxFeCoNi high entropy alloys. International Journal of Engineering Research in Africa, Trans Tech Publications, Switzerland. 2018;**37**:23-28. ISSN: 1663-4144

[13] Ştefănoiu R, Geantă V, Voiculescu I, Csaki I, Ghiban N. Researches regarding the influence of chemical composition on the properties of AlxCrFeCoNi alloys. Revista de Chimie. 2014;**65**(7):819-821

[14] Geantă V, Voiculescu I, Ştefănoiu R, Savastru D, Csaki I, Patroi D, et al. Processing and characterization of advanced multi-element high entropy materials from AlCrFeCoNi system. Optoelectronics and Advanced Materials—Rapid Communications. 2013;**7**:11, 874-12, 880

[15] Voiculescu I, Geantă V, Ştefănoiu R, Patroi D, Binchiciu H. Influence of the chemical composition on the

microstructure and microhardness of AlCrFeCoNi high entropy alloy. Revista de Chimie (Bucharest). 2013;**64**(12):1441-1444

[16] Geantă V, Voiculescu I, Chereches T, Zecheru T, Matache L, Rotariu A. Behavior to dynamic loads of composite multi-layer structures. Mats, Plastic (Bucharest). 2019;**6**(2):460-465

[17] Geantă V, Chereches T, Lixandru P, Voiculescu I, Stefănoiu R, Dragnea D, et al. Virtual testing of composite structures made of high entropy alloys and steel. Metals. 2017;**7**:496

[18] Geantă V, Chereches T, Lixandru P, Voiculescu I, Ștefănoiu R, Dragnea D, et al. Simulation of impact phenomena on the composite structures containing ceramic plates and high entropy alloys. ICIR Iasi, International Conference on Innovative Research-ICIR EUROINVENT 2017 IOP Publishing IOP Conference Series: Materials Science and Engineering. 2017;**209**:012043

[19] Csaki I, Ștefănoiu R, Geantă V, Voiculescu I, Sohaciu MG, Soare A, et al. Researches regarding the processing technique impact on the chemical composition, microstructure and hardness of AlCrFeCoNi high entropy alloy. Revista de Chimie (Bucharest). 2016;**67**(7):1373-1377

[20] Chereches T, Lixandru P, Geantă V, Voiculescu I, Dragnea D, Ştefănoiu R. Layered structures analysis, with high entropy alloys, for ballistic protection. IMANE Iași 2015. Applied Mechanics and Materials. 2015; **809-810**:724-729. ISSN: 1662-7482